

# Wide Tank Efficiency Measurements on a Model of the Sloped IPS Buoy

S H Salter    S.Salter@ed.ac.uk  
Chia-Po Lin    chiapo@holyrood.ed.ac.uk

Department of Mechanical Engineering, University of Edinburgh EH9 3JL, Scotland  
Tel +44 131 650 5703. Fax +44 131 650 5702

## Abstract

The idea for limiting the drive stroke of the Swedish Inter-Project Services (IPS) tail-tube buoy (Bergdahl 1992) by widening the passage in which a water piston moves, gives very attractive overload protection. At the Lisbon conference in 1995 we suggested that adjusting the angle of movement of an IPS buoy with an asymmetric head would improve performance. The slope constraint would be achieved by enclosing a number of the IPS tail tubes in a wide planar construction which would be long enough to reach down to calm water. The device would have very large added mass in the direction perpendicular to the slope plate but retain the hydrodynamics of a smaller buoy in the direction parallel. This paper presents test results which show the hoped-for effects.

## 1.0 The models

Figure 1, from our previous paper, shows a side view of the proposed full-scale device with the water piston coupled to a double-acting hydraulic ram. Video records of an unpowered freely-drifting model and model with a slack inclined mooring, made from polystyrene and light alloy sheet, show the successful operation of the slope-plate constraint - at least in short and medium wave lengths. They also confirm that we can achieve a stable flotation angle despite the rather short waterline.

In order to allow comparisons with existing theoretical analysis, the first powered model, shown in figure 2, was a half cylinder 0.3 metre in diameter and 0.5 metre in width with sharp corners. It was mounted on a slide of adjustable angle using hydrostatic bearings fed with tap water. The polystyrene buoy head was pierced with tubes to carry ballast weights which brought the water line to half the cylinder volume.

As in previous Edinburgh model tests the power takeoff was via a peizo-electric load cell to a carbon fibre thrust rod and then through pinch rollers to a printed armature motor using the design developed by Richard Yemm. The signal from a tacho-generator on the motor was amplified and used to oppose the movement of the buoy through an adjustable gain control to set damping. Power is calculated from the product, with regard to phase, of force and velocity. The model can also be driven by the motor as a wave maker allowing measurements of the ratio of force to velocity and their relative phases.

## 2.0 Force and impedance tests

Figure 3 shows the force on a fixed buoy head against wave height for a selection of wave periods. Force rises at slightly less than the first power of wave amplitude. We expect that the divergences will be reduced with future, more rounded models. At larger drive amplitudes there was very obvious vortex shedding at the sharp corners.

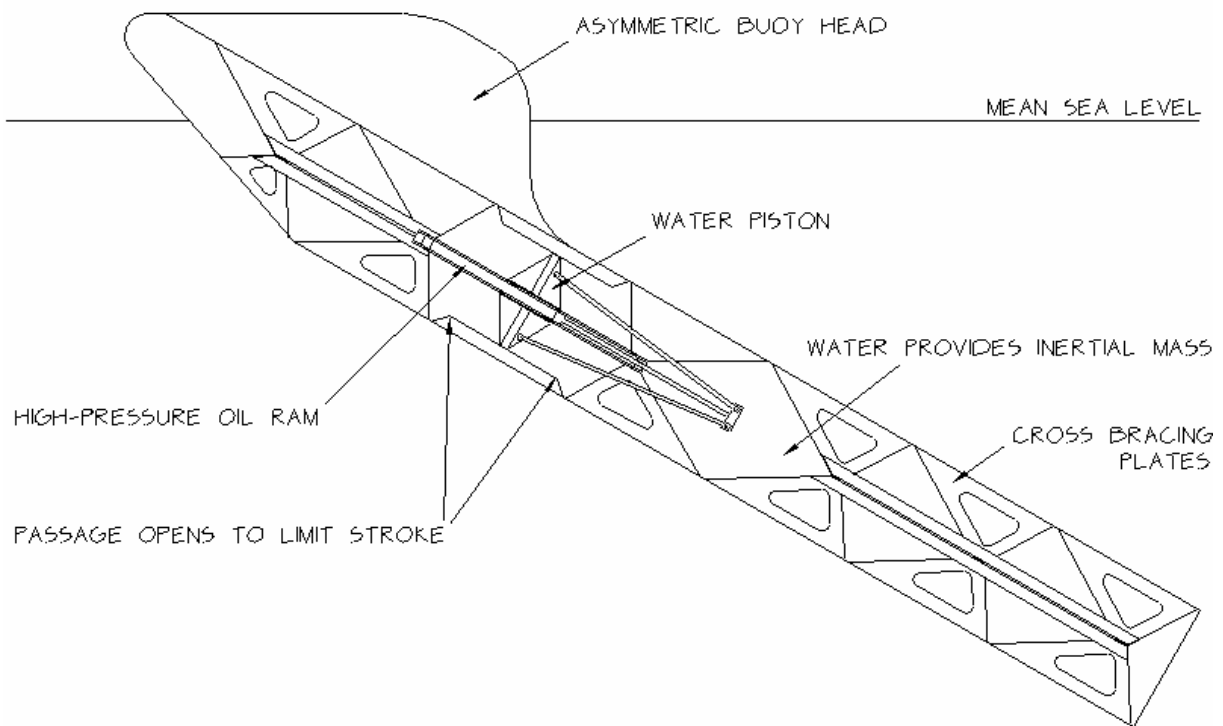


Figure 1. A sketch of the full scale device.

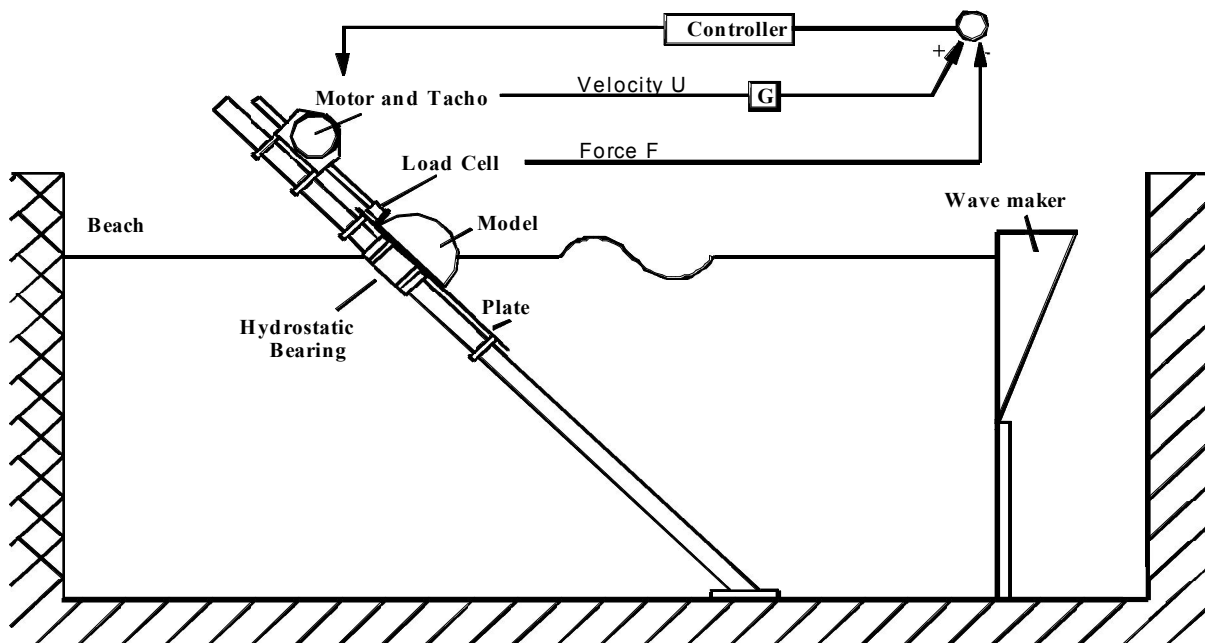


Figure 2. Schematic of experimental set-up in wave tank and the control loop of power takeoff system.

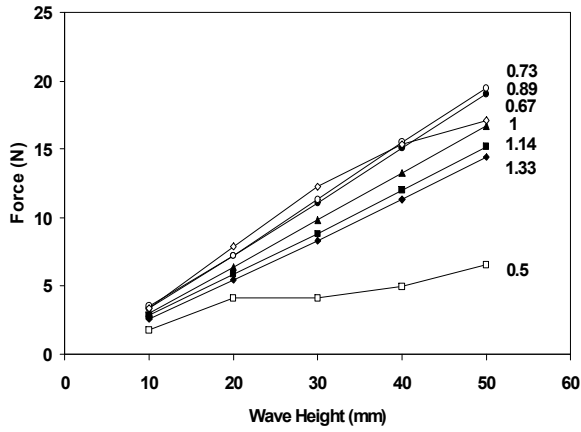


Figure 3. The wave excitation forces for different wave periods versus wave height for the latched model at 45 degree inclined angle.

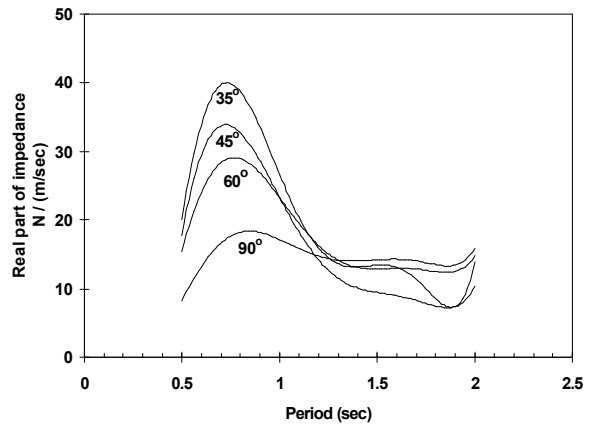


Figure 5. The real part of the impedance of the model for different angles of inclination

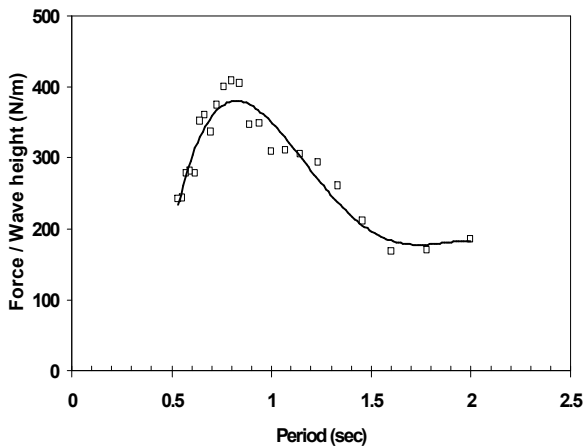


Figure 4. The wave excitation force coefficient versus incident wave periods for the latched model at 35 degree inclined angle.

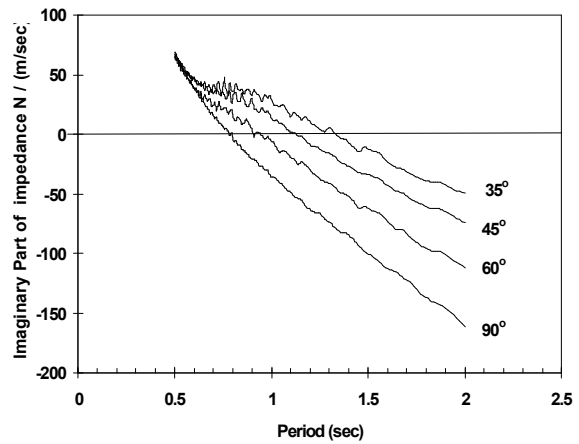


Figure 6. The imaginary part of the impedance of the model at different angles of inclination. The zero value of impedance corresponding to the natural periods.

Figure 4 shows the force against period on a fixed buoy head for the moderate wave height of 20 mm htc.. Figure 5 shows the real part of the ratio of force to velocity when the buoy head is driven in calm water as a wave maker for a number of slope angles. This is the total combination of friction with radiation and diffraction impedance.

Of particular interest is the effect of slope angle on the imaginary part of the impedance shown in figure 6. The small jags are the results of tank reflections and are repeatable for a given point in the tank. They are closer at shorter wave periods and move in expected ways for other test points.

At the top left of the diagram the impedance is dominated by inertia and all slope angles have the same mass. At long periods at the bottom right of the diagram the impedance is set by buoyancy spring rate and is reduced by slope. The device is at resonance when the spring and inertia cancel one another. The periods at which this occurs can be changed from 0.8 seconds for a vertical buoy to 1.3 seconds for a 35-degree slope angle. If this were a 1/100 scale model the change would be a very good match to the useful parts of the Atlantic spectra.

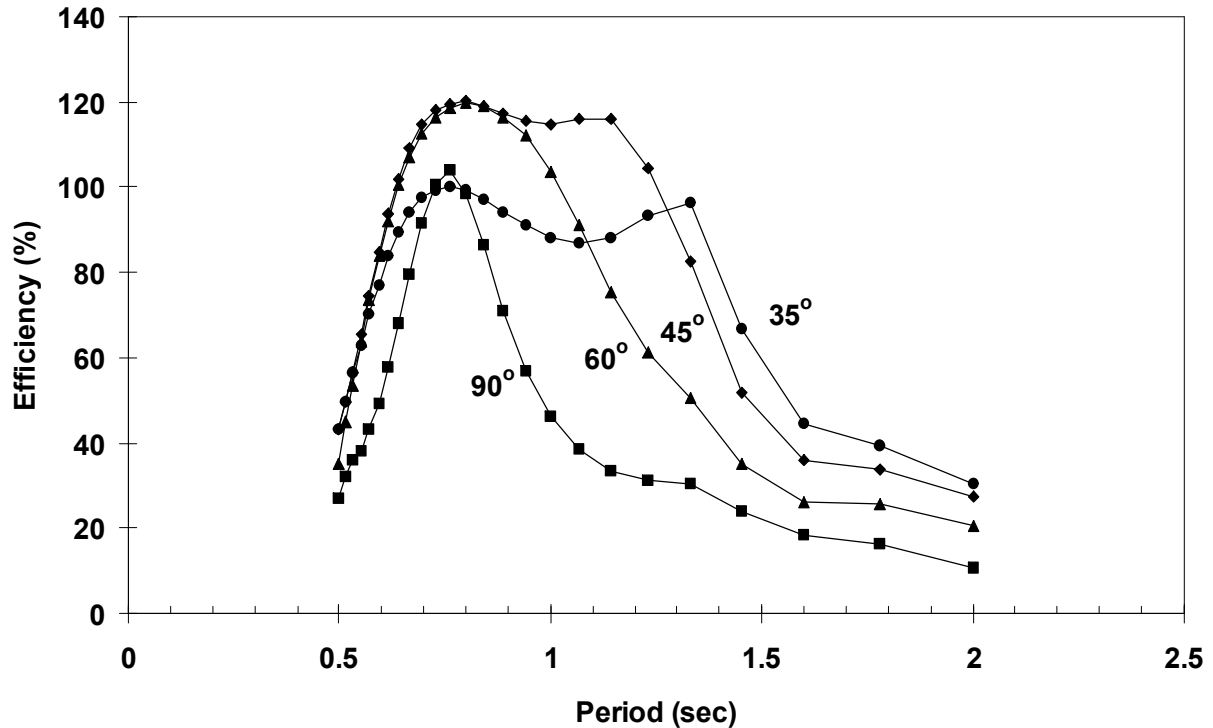


Figure 7. The theoretical efficiency curves for 35, 45, 60 and 90 degree inclined angles.

### 3.0 Efficiency measurements

The smoothed curves in figure 7 show the theoretical efficiency calculated (Evans 1981) from the impedance and excitation force results. At 12 seconds full scale the 45 degree slope would produce *four times* the output of a vertical buoy.

The 90-degree result should not be compared directly with that of normal heaving buoys because the asymmetry of the buoy head produces less wave generation on the lee side of the model and so should be more efficient.

Clearly the slope angles are having a profound effect in raising and widening the efficiency band over the most useful part of the spectrum. The 45-degree and even more the 35-degree slopes show signs of a double peaked efficiency curve with a wide plateau between 7 and 12 seconds period at full scale.

Slope even makes a small improvement at short period pushing the curve down in period by about a second. There is only a very small part of the spectrum, at 7.5 seconds, at which the 90-degree curve is slightly above the 35-degree one. We expect that the true efficiency

results will get closer to the theoretical ones if we reduce the vortex shedding induced at the sharp corners. From work on solo ducks we expect a rise of about 20% from this change.

The jagged curves in figure 8 are the actual efficiency values calculated from the product of force into a linear damper multiplied by the velocity measured by the tachogenerator. These are referred to wave sizes measured with a set of wave gauges placed at the model position with corrections for beach reflection.

### 4.0 Slope plate tests

All the data so far refer to just the head of the buoy which is sliding on a magic constraint but with no impediment to wave energy passing below the buoy head. We would expect the addition of a slope plate to prevent deep-water wave propagation and so help performance in longer waves. Figure 8 also shows the result of adding a fixed slope plate. Results are shown super-imposed on plain head ones. We can see that there is almost no change at short periods but a small gain in efficiency from 9 seconds and above.

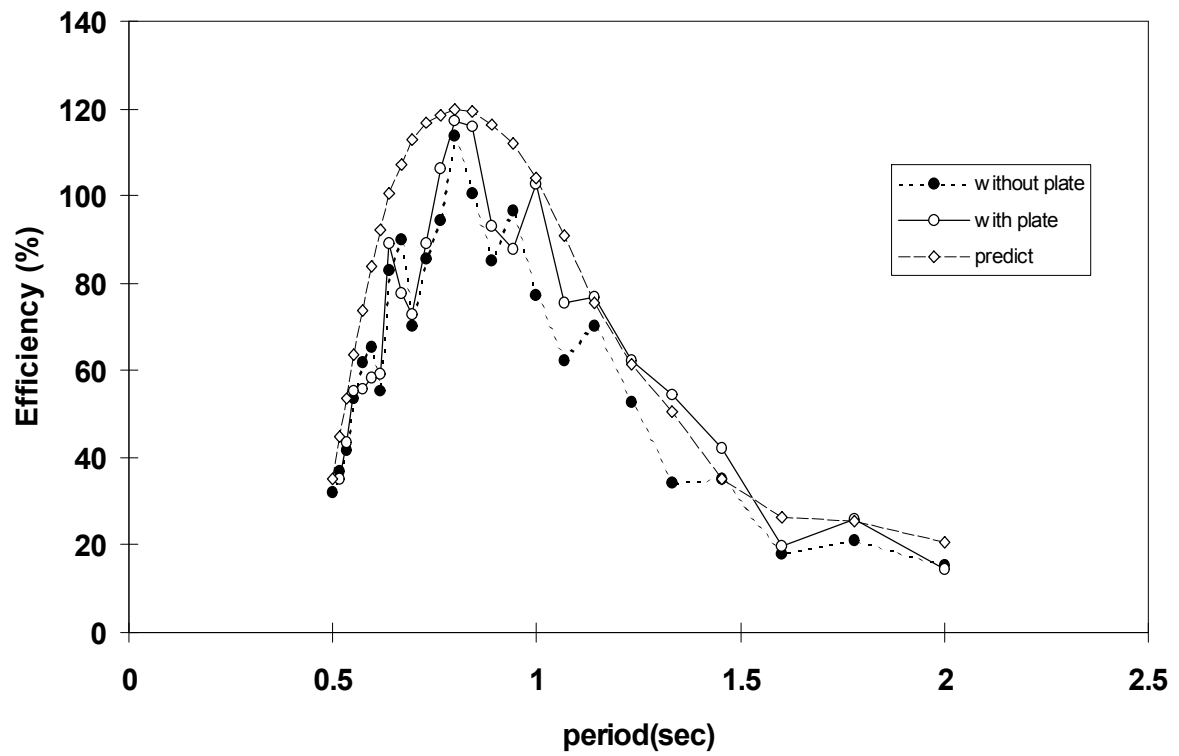


Figure 8. The 60 degree angle tests with and without fixed plate.

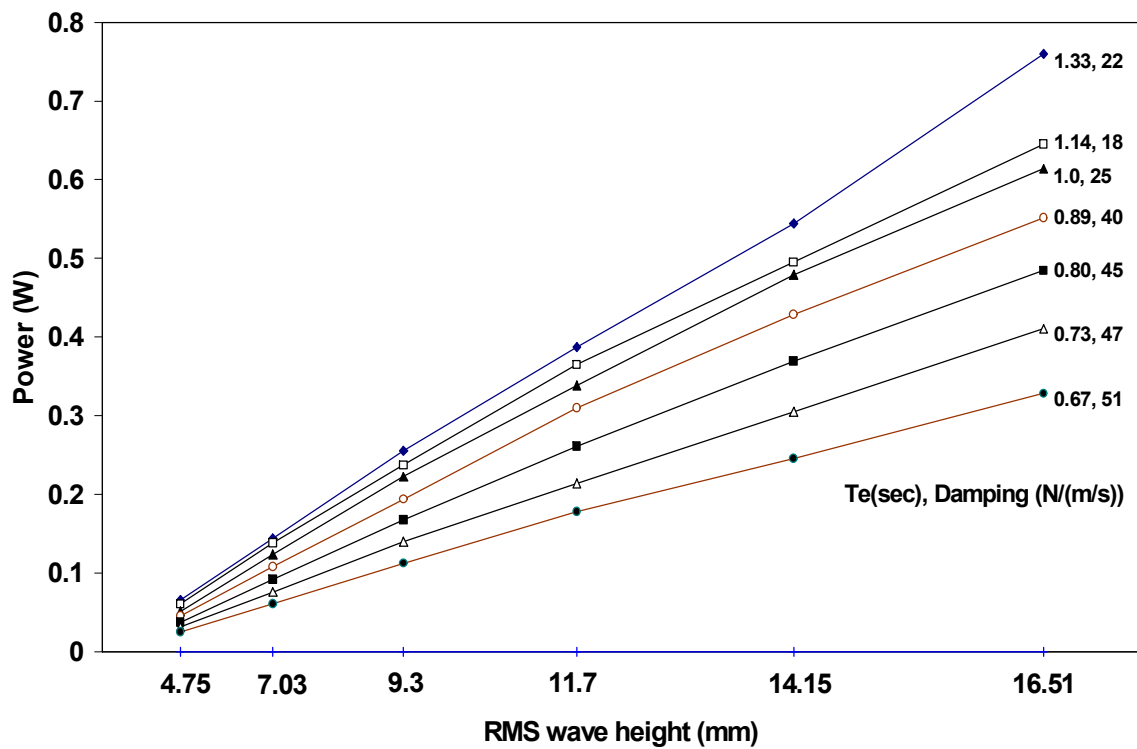


Figure 9. Power absorption for PM spectra at 45 degree inclined angle.

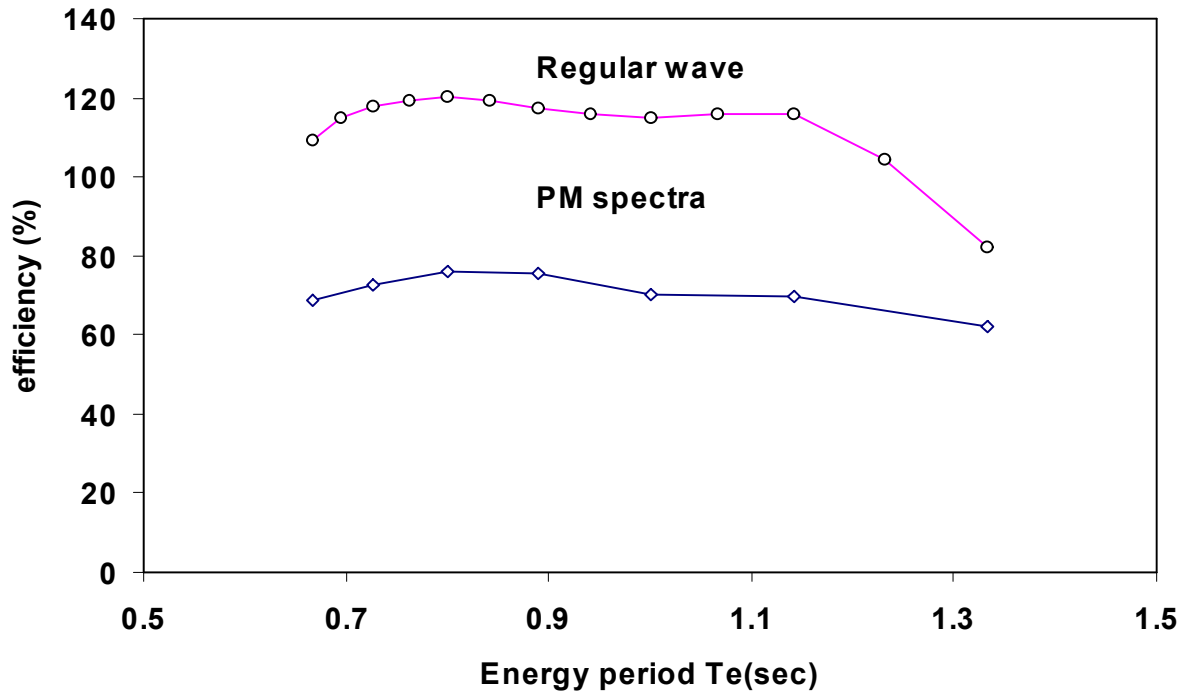


Figure 10. The efficiency curves for regular wave and PM spectra at 45 degree inclined angle.

### 5.0 Random wave tests

Figure 9 shows the results of tests in pseudo-random Pierson-Moskowitz spectra. Power is plotted against RMS wave height on a square scale. The device is fairly linear. Buoy motions are roughly double wave motions at the longer periods.

Figure 10 shows efficiency in long crested waves with an rms amplitude of 12 mm together with the regular wave results for the same amplitude

### 6.0 The next model

Tests on a correctly-powered, unconstrained device will require all the power take-off and instrumentation to be self contained and the mooring behaviour correctly represented. This will involve a much more elaborate model for which funds have not yet been raised. We propose the use of a fully immersed eddy-current sleeve located by hydrostatic bearings fed with tap water.

We must expect that an economically sized slope plate will have some surge movement which, depending on phase, will lose energy. However it might be possible to modify the shape of the leeward side of the model so as to generate the inverse of the waves generated by surge motion.

### 7.0 Full-scale cost estimates

We are indebted to David Taylor (1998) of Kier Construction for an initial analysis of costs of the first prototype. Using the folded steel plate in the triangular lattice described in our previous paper, the cost of an assembled and painted first prototype 'sea frame' without hydraulic-rams, motors and generation came to a total of £4.2m for a steel weight of 3000 tonnes. Power rating has not yet been decided but might be as high as 200 kW per metre width giving 10 MW maximum output from a 50 metre wide device.

Electricity costs for the entire system with installation and connections are being prepared by Thorpe and should be available at this conference.

While steel is very convenient for initial production runs and easy modifications, in future, it may be interesting to look at ferrocement because of the lower energy content and reduced corrosion problems.

Although most attention has been given to electricity generation, the deep-sea capability of the device makes it suitable for the near-term niche market of pumping water or gas into partially depleted oil strata so as to increase the fraction of oil recovered. Intermittent output would be acceptable.

## 8.0 Conclusions

- The sloped IPS buoy is an asymmetric, solo, deep-water, resonant, hard-skinned, slack-moored, potentially self-propelled, yard-built, wide point-absorber with high-pressure oil power conversion reacting to an internal water mass which can be disconnected at a chosen stroke limit.
- Slope plates can stabilise freely drifting and slack-moored models, at least in short and medium wavelengths.
- Changing slope angle raises and widens the efficiency of a buoy with gains of four times at useful parts of the spectrum. A single angle should cover most of the useful range so that we may not need seasonal trimming but it is possible to move resonance to any useful part of the Atlantic spectrum.
- Buoy motions are about twice water motions.
- The buoy seems very linear with excellent random wave results except for the shortest, directional seas.
- Further improvements may be achieved if we can reduce vortex shedding with rounded corners and allow a yawing motion. This should produce random sea capture widths above unity.

## References

- Bergdahl L. Review of Research in Sweden. Wave Energy Workshop, Cork. pp.129-136. 1992.
- Evans D. Maximum Wave-Power Absorption Under Motion Constraints. Applied Ocean Research, 1981 Vol.3 No.4.
- Pizer D. Numerical Modelling of Wave Energy Absorbers. University of Edinburgh Wave Power Project Report to DTI V03 00172 0000. 1994.
- Salter S, Lin C. The Sloped IPS Wave Energy Converter. 2nd European Wave Energy Conference Lisbon. pp. 337-344 1995.
- Taylor D. Personal communication 1998.
- Thorpe T. Economic Analysis of Wave Energy Devices. Paper at this conference. pp.